Development of Graphene Oxide Nanosheets as Potential Biomaterials in Cancer Therapeutics: An In-Vitro Study against Breast Cancer Cell Line

Yugal Kishore Mohanta (ykmohanta@gmail.com)
Maharaja Sriram Chandra Bhanj Deo University https://orcid.org/0000-0002-6547-7227
Kunal Biswas
Maulana Abul Kalam Azad University of Technology
Pradipta Ranjan Rauta
Shriram Institute for Industrial Research
Debashis De
Maulana Abul Kalam Azad University of Technology
Abeer Hashem
King Saud University
Abdulaziz A. Alqarawi
King Saud University
Elsayed Fathi Abd-Allah
King Saud University
Saurov Mahanta
National Institute of Electronics and Information Technology
Tapan Kumar Mohanta
University of Nizwa

Research Article

Keywords: Graphene nanosheets, DPPH radical, H2O2 assay, MDA-MB-231, HaCaT, Transmission electron microscopy, Scanning electron microscopy

Posted Date: April 7th, 2021

DOI: https://doi.org/10.21203/rs.3.rs-385884/v1

Version of Record: A version of this preprint was published at Journal of Inorganic and Organometallic Polymers and Materials on August 16th, 2021. See the published version at https://doi.org/10.1007/s10904-021-02046-6.

Abstract

Recent advances in nanotechnology and nano biomaterials have attracted considerable attention in the field of cancer therapy. The development of biocompatible nanotherapeutics that selectively target cancer cells is a prime area of interest and current research. The use of graphene is being explored in a variety of sciences, ranging from electronics to biomedical fields. In the present study, graphene oxide nanosheets were synthesized using a modified Hummer's method. FTIR spectroscopy, Raman spectroscopy, and X-Ray Diffraction analyses were used to characterize the as-synthesized nanosheets. FE-SEM and HR-TEM were also used to examine the structure of the as-synthesized nanosheets. Surface topography and thickness measurements were also conducted by Atomic Force Microscopy. Results indicated that the lateral thickness of the graphene nanosheets was approximately 6.45 nm, which was corroborated by the TEM and AFM analyses. Characteristic defect peaks observed in Raman spectroscopy and electron microscopy images along with the respective EDAX calculations confirmed the formation of graphene nanosheets. The potential biomedical application of graphene nanosheets was evaluated by assessing the cytotoxicity of the graphene nanosheets against human breast adenocarcinoma [MDA-MB-231] and HaCaT normal cell lines. Two different *in-vitro,* anti-oxidant activity assays of Graphene Oxide [GO] were employed, namely DPPH radical and the H_2O_2 scavenging activity. Antioxidant activity of GO was assessed in a measured concentration-dependent manner to better understand the cytotoxicity of the GO sheets in the different cell lines. The *in-vitro* tests revealed that the GO sheets had a high level of cytotoxicity to the human breast cancer MDA-MB-231 cells that was concentration dependent. In contrast, the cytotoxicity of the GO sheets against the HaCaT normal cell line was marginal, suggesting that the graphene nanosheets could be safely used in cancer therapy.

1. Introduction

The novel and fascinating properties of graphene-based materials suggest that these materials may have many potential biomedical applications [1]. Graphene oxides are a class of nano-materials in the size range of 1-100 nm and fall into a category of two-dimensional carbonaceous nanomaterials with dimensions of approximately a few nanometers in thickness. Owing to the unique physio-chemical properties of graphene oxide (GO), including the available surface oxygen groups, GO can form a stable suspension in different solvents, indicating its hydrophilic nature within the family of carbonaceous nanomaterials [2]. Due to the presence of a unique surface to volume ratio, along with surface properties such as a huge concentration of surface atoms, augmented surface energy value, and other characteristics, makes GO a suitable candidate for a myriad of applications. Potential applications range from biomedical applications (viz. drug delivery, protein therapy etc.) and bioengineering (biosensors and bioimaging) to anti-microbial therapy and bioengineering (scaffolding of tissue) [3, 4]. Due to its high surface to volume ratio, GO sheets provide a reactivity and adsorption platform for other biological macromolecules enabling bioprocesses to occur at a nanoscale level that are mesoscopic in nature [5]. The probability of redox reactions between the material and a biological system due to the free electrons

present on the surface of graphene oxide sheets, increases the number of potential applications of carbonaceous nano-materials in biological systems [6].

Nanobiotechnology has emerged as a promising platform for employing nanomaterials in the field of cancer biology [5]. Due to the unique physio-chemical properties of the nanomaterials, the same could be used for targeted drug delivery for bearing the outcompeting behavior of natural delivery mechanisms such as reaching the nuclear membrane and penetrating it for delivery in the proteins and the DNA sequences [3]. Graphene oxide [GO] has been recently proposed as a good agent in cancer therapeutics and diagnosis [7]. The morphology and the viability of the glioma cells U87 and U118 respectively, have been shown to be less effective from the treatment of GO sheets [8]. Also, Chang et al., [2011] has studied the adverse effect over the A549 cells due to the generation of oxidative stress by GO. It has also been reported that GO sheets bring significant damage to the mitochondrial membrane, resulting in altered mitochondrial potential [10]. Compared to other nano-scaled nanomaterials, such as gold and silver nanoparticles which are used in different medical therapies, carbonaceous materials like GO have lesser deleterious intrinsic activity in the drug delivery process of DNA, RNA for achieving targeted drug delivery mechanism [11, 12]. The great convenience of using graphene oxide [GO] over other carbon-based materials is due to its aqueous dispersibility and colloidal stability in both single or few-layered GO. As a result, these materials are becoming immensely popular as novel tools in the biomedical field[13].

The surface properties of pristine graphene oxide and graphene sheets increases their overall potential for activity within biocompatible applications [14]. In this regard, an interaction between GO sheets and targeted ligands in lung epithelial cells [15], neuronal cells [16] and fibroblast cells has been reported [Gao et al, 2012]. Furthermore, the use of GO sheets in conjunction with sulfonic acid in drug delivery systems makes the GO suspension more stable, while decorating the sheets with folic acid molecules has been used to target human breast cancer cells with folic acid receptors [17]. Folic acid-conjugated GO sheets have been employed for the delivery of anti-cancer drugs, such as doxorubicin and calprotectin, into tumor cell lines with great success in MGC803 cells [18]. Yang et al., 2010 reported that a higher rate of uptake in tumor cells and *in-vivo* photothermal therapy was achieved by using PEGylated Graphene sheets in a mouse model subjected to an ultra-low power laser injection of $2Wcm^{-2}$. The interaction of graphene with DNA/RNA macromolecules favors the use of GO sheets over GO alone, due to the presence of the carboxylic, hydroxide, and epoxy groups present in GO sheets, which provides greater potential bioactivity and thus, greater potential application in a wide range of biomedical fields and bio-macromolecular systems [14]. The higher rate of drug adsorption to hydrophobic materials also makes GO a preferred choice amongst the graphene family of nano-scaled materials, such as graphene, rGO (large GO), and others [19]. Extensive studies of graphene-based materials for different biomedical applications have fostered nano-biomaterial development for practical use and commercialization.More studies on graphene are required, however, to achieve safe and effective commercial applications of this technology.

In this present study, the Hummers method, with some modifications, such as the use of sulphuric acid [H_2SO_4], and varying the Graphite: $KMn0_4$ ratio in the reaction mixture, was used to optimize GO

production. The cytotoxic activity of the GO nanosheets against the MDA-MB-231 breast cancer cell line was also evaluated, along with its effect on a normal, HaCaT cell line. During the application of any foreign biomaterials, there is the potential of inducing oxidative stress. Therefore, the DDPH radical and peroxide scavenging assays were also conducted. Results of the study indicate that oxidation plays a key role in the activity of GO nanosheets in biological systems.

2. Material And Methods

2.1. Preparation of GO nanosheets

GO nanosheets were prepared using the commonly-used method described by Zaaba et al. [2017]. Graphite powder was subjected to chemical exfoliation using a modified Hummer's method. Briefly, 1.5 g of sodium nitrate [MERCK] were mixed with 2 g of graphitic powder [purchased from Sigma Aldrich]. The resulting powdered mixture was then placed in 75 ml of 98 % H_2SO_4 and stirred for 48 hr. The solution was then placed at 10°C for 12 hr, after which 10 g of $KMnO_4$ powder was mixed in. The mixture was then placed in a 0°C ice bath for 15 min. After this, the solution was heated to 35°C on a hot-plate. Subsequently, 140 ml of deionized water [DI] was added to the solution during which time the exothermic reaction occurring in the solution raised the temperature of the solution to ~ 98 ℃. The temperature of the solution was then lowered by placing the reaction solution in a 35℃-water bath for 20 minutes. The color of the solution began to change from black to brown, indicating that a chemical exfoliation process was occurring in the solution at a nano-scale level. After 25 minutes, 450 ml of DI water and 10–15 ml of 30 % H_2O_2 was added to the solution. The solution then took on a yellowish hue, indicating the synthesis of GO sheets. The solution was then centrifuged and the precipitate was collected and washed with 37% HCL, followed by a second washing with DI water. The pH of the solution was maintained at a pH of 7.0. The GO slurry was then poured into a fresh container for further use. The GO slurry was used to characterize the GO sheets and to prepare a dry powder by air drying the slurry in an oven at 90^0C for 24 hours.

2.2. FT-IR spectroscopy

The FT-IR spectra of dried samples of GO sheets were identified and recorded using a Perkin-Elmer spectrum RX-1 IR spectrophotometer. The analysis of the GO sheets was performed by preparing the powdered samples into a KBr pellet, drying the pellet, and subsequently subjecting the dried pellet to ATR-attenuated FT-IR at 4500 – 500 cm^{-1}. Different functional groups against a specific inverse peak of wavenumber [cm^{-1}] were calculated to identify specific functional groups present in the structure of the GO sheets.

2.3. Raman spectroscopy

The powdered samples of GO sheets were analyzed by Raman spectroscopy to identify any aberrant proportions in its structure by calculating the I_D/I_G ratio, which is a hallmark signature of any carbonaceous nano-materials. An Ar + ion laser at an excitation wavelength of 514 nm was used and the

vibrational modes of the intrinsic structures were studied using Lab Ram HR800 micro-Raman spectroscopy [Horiba Jobin-Yvon, France].

2.4. X-Ray Diffraction [XRD] of GO sheets

The powdered samples were subjected to XRD [Bruker Advance D8] with a Cu Kα [λ = 1.5406 Å] to determine the crystalline structure and lattice planes in the material.

Different lattice planes against specific diffraction angles were calculated and used to determine the intrinsic details of the structure based on the diffractogram.

2.5. FE-SEM [Field Emission Scanning Electron Microscopy] of GO

The surface topography of the powdered GO sheets was observed using FE-SEM [EVO-60, Zeiss company]. The powdered samples of GO sheets were drop-casted on to the surface of a glass coverslip and dried overnight. The resulting samples were viewed under an FE-SEM at an operating voltage of 20 kV. The particle size of the GO sheets was calculated using a technique for determining the layer thickness and the particle diameter based on the use of a raster scanning mode.

2.6. HR-TEM [High Resolution-Transmission Electron Microscopy] of GO

For the HR-TEM analyses, the powdered samples were deposited on carbon-coated, copper grids [300 mesh size, regular grip, spi 2030 C] and allowed to dry overnight. The resulting samples were viewed in HR-TEM [FEI-TECNAI G2 2OS-TWIN, Netherland] at a frequency of 80 Hz.

2.7. Atomic Force Microscopy of GO

AFM [Bruker AXS Pte Ltd, Innova] was used to examine the surface properties of the GO sheets at a differential electrostatic charge distribution [in mV] using a cantilever-based deflection. The sample was prepared by drop-casting slurry onto a silicon wafer and allowing the samples to dry prior to examination by AFM.

2.8. DLS [Dynamic Light Scattering] of GO

The particle size and zeta-potential of the powdered GO sheets at room temperature were analyzed using a Zetasizer [Zs-90, Malvern, UK]. The dried samples were first adequately diluted in Phosphate Buffer Saline solution [0.15 M, pH 7.2]. Aliquots of the GO suspensions, at a concentration of 10 µg/ml from a stock [1mg/ml], were subjected to further analysis under DLS. Particle size distribution was determined at a scattering angle of ~ 90ºC.

2.9. Antioxidant Activity

The anti-oxidant potential of GO sheets was evaluated based upon a measurement of resistant DPPH free-radical scavenging. Briefly, 1.9 ml of a methanol solution of DPPH [0.004%], and 0.1 ml of different

concentrations of GO, were mixed together. The solution was then mixed robustly and kept for 30 min in the dark. Absorbance of the solution at 517 nm was then determined by using a Shimadzu UV-1280 spectrophotometer. The addition of ascorbic acid to DPPH was used as a control. All tests were performed in triplicate. The ability to scavenge DPPH radicals was calculated by using the following Equation [1]:

Ability to scavenge DPPH [%] = [AO − A1]/A0] × 100 (1)

In the equation, AO is the absorbance of the control, while A1 is sample absorbance.

H_2O_2 scavenging activity of the GO sheets was also determined using a slightly modified Ruch Figure method [16]. Briefly, a 40 mM H_2O_2 solution was prepared in 0.05 M KH_2PO_4-K_2HPO_4 phosphate buffer [pH = 7.4]. Various concentrations of GO were then added to the prepared H_2O_2 solution (1.4 ml phosphate buffer and 0.6 ml 40 mM H_2O_2). The absorbance of the H_2O_2/GO solution was then measured after 10 min at 230 nm using a Shimadzu UV-1280 spectrophotometer, and used to estimate the concentration of H_2O_2. Ascorbic acid, instead of the GO solution, was used as a positive control. All tests were performed in triplicate and H_2O_2 scavenging ability was calculated by using Equation [1].

2.10. Cytotoxicity and biocompability with different cell lines

2.10.1. Cell Culture

The cell lines chosen for the cytotoxicity assay were a human skin HaCaT and a breast cancer cell line [MDA-MB 231]. The basal medium used for all cell culture experiments was Dulbecco's Modified Eagle's medium supplemented with 10% Fetal Bovine Serum, and streptomycin sulfate and benzyl antibiotics at a final concentration of 100 µg/ml and 100 U/ml, respectively. Cell cultures were maintained at 5% CO_2 and 37°C throughout all the experiments. The cells were passaged using 0.25% Trypsin-EDTA at around 80% confluence. Cells were seeded in 96-well plates at a density of 5×10^3 cells/well for the MTT assays.

2.10.2. MTT Assay

Cytotoxicity and biocompatibility was assessed using an MTT colorimetric assay at 24 and 48 hour after incubation of the cell lines with the GO nanosheets [21]. Doxorubicin was used as a positive control. A stock solution of dimethylthiazolyl-diphenyltetrazolium bromide [MTT; 1mg ml^{-1}] in PBS was prepared immediately prior to use. A 500 µl volume of the MTT solution [50µg ml^{-1} MTT in culture medium] was added to each culture dish without a cover. Cells were incubated for 3 h, and reduced formazan was then extracted with 500 µl DMSO and absorbance was measured at 570 nm in a spectrophotometer. Cell survival was expressed as the percentage of absorption of treated cells in comparison with untreated, control cells.

2.11. Statistical Analysis

Each assay was performed in triplicate to ensure reproducibility. The results of the antioxidant assays were expressed as a percentage of inhibition, while the cytotoxicity results were expressed as percent viability, relative to the control. Values obtained in the antioxidant and cytotoxicity assays for the different treatment groups vs. the controls were statistically evaluated using a Student's t-test ($p \leq 0.05$).

3. Results And Discussion

3.1. Characterisation of GO sheets

3.1.1. Fourier Transform Infra-Red Spectroscopy

The GO nanosheets were evaluated prior to their use in the *in vivo* bio-application studies. The structure and possible function of individual molecules were evaluated to better link activity of the GO nanosheets with its structural components. Prior knowledge of the molecules and bonding pattern could also help to predict expected outcomes in the use of the GO nanosheets. The FT-IR spectra of the architecture of GO sheets [Figure 1] revealed the presence of the characteristic wave-numbers of 1585 cm^{-1}, 2841 cm^{-1}, and 3443 cm^{-1}. These wave numbers represent the functional groups linked to the structure of the GO sheets, and reveal the presence of C = C, C-O, and C = O bonds, respectively. The wave number present at ~ 1096 cm^{-1} is associated with both C-C and C-O bonds. The broad signal observed around 3443 cm^{-1} indicates the O-H bond vibration of the hydroxyl groups present in the GO architecture [22].

3.1.2. Raman spectroscopy

Raman spectroscopy is an important analytical tool that provides both qualitative and quantitative data on nanomaterials based on its chemical composition and structure [23]. The Raman plot [Figure 2] contains the I_D/I_G ratio of ~ 1.05, which is characteristic of powdered GO sheets. The defect ratio represents the compromised proportion and lesser quantified nature of the available defects present in the GO sheets. More specifically, it indicates the presence of a slightly lower number of dangling bond associations in the native structure of the GO sheets, compared to the previously reported graphene sheets of rGO forms that have a value of 1.35. Such observations indicate a more conductive nature for GO forms, relative to its other counterparts [Graphene, rGO, etc.], making it suitable as an inhibitory anti-cancerous agent that can be used against a variety of cancer cells.

3.1.3. X-ray Diffraction

The X-Ray Diffraction [XRD] analysis [Figure 3] revealed the presence of lattice planes that are characteristic for powdered GO sheets. Notably, 001 and 002 lattice planes at a diffraction angle of 30° were evident. These characteristic lattice planes indicate the nature of the available crystallinity of GO

sheets. The polycrystalline nature of GO sheets is evidence that such lattice planes are present and were corroborated by the TEM SAED pattern.

Thermo-gravimetric analysis (TGA) is a method of thermal analysis in which the physical and chemical properties of materials are measured as a function of increasing temperature (with a constant heating rate), or as a function of time (with constant temperature and/or constant mass loss). TGA contrasts with DTA, where the material under study and an inert reference undergo identical thermal cycles, and differences in the temperature between a sample and reference are recorded[24]. Results indicated that exposing the as-prepared GO materials to temperature changes affected its exposure. The physico-chemical properties of the GO sheets were altered by changes in temperature and defects were induced in the structure of the material, which was corroborated by the Raman defect ratio (ID/IG) of the material.

3.1.4. FE-SEM Analysis

Field emission scanning electron microscopy provides information on the surface topography and composition of nanoscale materials [24]. Data on the surface morphology is highly useful regarding the potential use of the nanomaterials in medical devices and for other applications. The typical surface topography of GO sheets was evident in the FESEM analysis (Fig. 4). Surface undulations were evident in GO sheets (Fig. 4A), as well as rough edges. Undulations and rough edges are the result of reaction kinetic phenomenon resulting in reduction and oxidation processes during the production of the GO powders. Energy Dispersive X-Ray Spectroscopy (EDAX or EDS) at a characteristic energy (keV) was used to evaluate the intrinsic chemical constituents of the as-prepared GO sheets (Fig. 4b). As evident in Fig. 4B, carbon (C) and oxygen (O) make up the major proportion of the as-prepared GO sheets. The EDS results indicate that during the synthesis of the GO sheets from its precursor graphite compound, various reducing agents and other chemical constituents used in its preparation, as well as solvents such as H_2SO_4, are present as trace amounts of sulphur (S), while the traces of silicon (Si) been originated from the silicon substrate of the grid used to examine the GO sheets in the FE-SEM.

3.1.5. HR-TEM Analysis

The primary purpose of the High Resolution – Transmission Electron Microscopy (HR-TEM) analysis was to observe high magnification images of the internal structure of the GO sheets and gather information related to the crystalline structures, internal fractures, stress, and contamination of the test sample. Information on the internal structure allows one to have greater confidence in the potential application of the nanomaterial and predict potential effects on the target system [25]. HR-TEM observations indicated that the internal structure of the prepared GO sheets possesses a folded morphology (Fig. 5). The presence of undulating folds and rough edges in the carbon sheets are evidence of the successful synthesis of GO sheets as previously noted by several authors. HR-TEM imaging enables one to visualize the internal, structural architecture of the prepared GO sheets, which is not possible by FE-SEM. In contrast, HR-TEM provides a clear picture of the internal structure of GO sheets at a resolution of 2 microns. The layers of the GO sheets, resulting from the reduction and oxidation processes occurring during GO synthesis, can be readily seen in Fig. 5. The lateral thickness of the GO sheets was ~ 9 nm.

Selected Area Electron Diffraction (SAED) is an attachment to HR-TEM system of imaging that provides information on the underlying crystalline properties of the examined samples. SAED analysis of the powdered GO sheets revealed the characteristic polycrystalline nature of the samples (Fig. 5b). The results of the SAED analysis are in agreement with the results obtained in the X-ray Diffraction (XRD) analysis, both of which have revealed the polycrystalline structure of the GO sheets, due to its crystalline lattice planes (Fig. 3). Thus, SAED studies complement X-ray Diffraction studies for the examination of GO nanomaterials.

3.1.6. AFM Analysis

In the application of a nanoscale material in living systems, local properties of a sample, such as height, friction, and magnetism, should be carefully assessed. The atomic force microscopy (AFM) analysis conducted in the present study provided information needed to determine its suitability for use in different bio-applications. Rough undulations at different tapping voltages of the AFM tip can be observed in Fig. 6. The thickness determined by AFM was in agreement with the results obtained in the HR-TEM analysis of the GO sheets. The charge distribution of the sheet at different electrostatic voltages is indicated by the colored bar graph.

3.1.7. DLS measurements of ζ-Potential

GO exhibits a ζ- potential of -29.3 mV, which is thought to be the most colloidal stable form [Figure 7]. An augmented cytotoxic effect against cancerous cells is observed by GO sheets due to its surface anionic charge. The percolation tendency of GO sheets may be attributed to the average size and overall tension occurring in the membranes of cancerous cells, which ruptures the membrane and allows entry of the material into the cell [26]. Endocytosis appears to be the prime mechanism underlying the entry of GO sheets into cells, however, further validation is required to confirm the mechanism by which GO sheets enter and exit living cells [27]. The interface of GO sheets with biological cells is also attributed to the electrical disruptions that occur at the material-bio interface. In this regard, the dimensions, size, shape, and intrinsic chemical composition of GO sheets play a significant role in the net cytotoxicity of the nanoparticles in biological systems [28].

The DLS analysis was repeated three times and a statistical significance of $p \leq 0.05$ was achieved for the repeatability of the experiments using a student's- t test. Colloidal stability of the GO was observed, which determines the surface charge of the powdered GO sheets. The average colloidal stability of the material was determined to be ~ 29.3 mV.

The experimentation has been repeated thrice and the statistical significance of $p \leq 0.05$ has been achieved for the repeatability of the experimentations using students- t test. Colloidal stability has been observed in this study which determines how much is the surface charge existing over the powdered sample when experimented. The average colloidal stability of the material came to be ~ 29.3 mV upon triple repetition of the experimentation.

3.2. Anti-oxidant Assays

As indicated by previous studies, there are various types of nanoparticles that can function in free radical scavenging and act as antioxidant agents [29, 30]. The antioxidant properties of the prepared GO sheets were analyzed using the DPPH radical scavenging assay and an H_2O_2 assay. Results indicated that the free radical scavenging activity of GO sheets was concentration dependent [Figure 8], with scavenging activity increasing as the concentration of GO sheets increased from 25–400 µg/ml. The IC_{50} value was 105.82 ± 1.78 µg/ml. The mechanism of DPPH radical scavenging is achieved by the donation of hydrogen to the free radicals [32]. H_2O_2 radical scavenging activity was concentration dependent (Fig. 9). The IC_{50} of H_2O_2 scavenging activity by GO sheets was determined to be 61.91 ± 1.14 µg/ml. The intrinsic cytotoxicity of H_2O_2 is due to the release of OH- as H_2O_2 is not in itself reactive in nature. Therefore, any treatment regime employing the H_2O_2 assay needs to be carefully examined when dealing with the interface with biological systems, specifically liver cells *in vitro*. The use of a graphene-based treatment [graphene, rGO, and GO] in the biological systems helps to counterbalance the free radicals generated as a side effect of the peroxide assay in biological systems. This needs to be taken into account when measuring cytotoxicity and antioxidant activity of graphene-based compounds in biological systems. The antioxidant activity of GO sheets is based on the overall physico-chemical properties of the GO materials [31]. The formation of the radical adduct at the sp^2 carbon sites determines the antioxidant activity of carbonaceous nanomaterials. The minimization of free radicals generated in H_2O_2 assays is also mediated by the formation of the second adduct leading to the donation of free radicals and a chelation system, thereby inhibiting the Fenton-based free radical system making GO-based antioxidant activity more prominent and significant [30, 32]. Based on the results of the DPPH and H_2O_2 assays, it appears that the GO nanosheets are safe for the development and use of biocompatible nanomaterials for different healthcare applications.

3.3. Microscopic studies of GO invasion

GO nanosheet and fluorescent protein [GFP] tagged-MDA-MB-231 cells were used to study the uptake of GO sheets into cells [Figure 10]. The cells were exposed to 100 µg/mL of GO for a period of 48 h., after which the cells were observed under a fluores fluorescence inverted microscope. Results indicated that clusters of nanoparticles appeared in close vicinity to and in the cytoplasm of GFP-MDA-MB-231 cells and was passively absorbed into the cells in a time-dependent manner.

3.4. Cell viability assay

The methylthiazolydiphenyl-tetrazolium bromide [MTT] assay was used to evaluate cell viability. Human keratinocyte (HaCaT) cells treated with GO sheets in culture for 24 hr at 37^0C were evaluated for cell viability [Figure 11]. Results indicated a concentration dependent effect of GO sheets on HaCAT cell viability. HaCAT cells exposed to 125 nM GO exhibited 99.26% level of cell viability. The viability percentage, however, slowly decreased as the concentration of GO increased. Exposure to 1000 nM GO

reduced cell viability of HaCAT cells to, 73.43%. These results confirm that GO is relatively non-toxic to normal cells as more than 50% of the cells were viable, even at a higher concentration. Therefore, it appears that GO nanosheets can be used for various potential biological applications due to its biocompatibility. The biocompatibility of GO with HaCaT cells has been previously demonstrated [33].

In contrast, the cytotoxicity assay of GO sheets with breast cancer cells [MDA-MB-231] revealed significantly higher levels of cytotoxicity [Figure 12 and Fig. 13]. Treatment of the cancerous cells with a ~ 1000 nM solution of GOS sheets for 24 h decreased cell viability to ~ 23.46 %. A time-dependent and dose-dependent cytotoxicity of GO nanosheets against MDA-MB-231 cells have been previously reported [34, 35].

The percentage of viable cancer cells decreased as the concentration of GO increased. The percentage of viable cells was 63.82% and 92.04% after treatment with 125 nM and 1.95 nM GO solutions, respectively. These results indicate that MDA-MB-231 (human breast cancer cells) exhibit a concentration dependent response in cytotoxicity. The cytotoxicity, however, did not appear to be time-dependent as a similar percentage of viable cells was observed after both 24 hr and 48 hr of incubation with the same concentration of GO sheets [Figure 9]. It is suggested that ROS production plays a role in the mechanism of cellular toxicity of GO sheets in human breast cancer cells [MDA-MB-231] [35]. GO toxicity in cellular systems is also determined by the biologically essential organelle, the mitochondrion, and the ROS that is generated and induces cellular apoptosis when a material, such as GO sheets, are introduced into a cell and disrupts metabolism [34]. In the case of treatment with doxorubicin [control], the IC50 values are higher in MDA MB 231 cells than HaCaT cells after both 24 h and 48 h of exposure. In contrast, the IC50 values for the GO treatment were significantly lower in MDA MB 231 cells than in HaCaT cells after both 24 h and 48 h of exposure [Figure 13].

4. Conclusion

The present study demonstrated the impact of GO sheets on the viability of breast cancer cells. It was shown that due to the rough edges, and the lesser number of available defects in the structure of the GO sheets, the level of cytotoxicity towards the cancerous cells was very strong. The morphology of the treated cells was also altered, relative to untreated cells, indicating that the cancer cells had been damaged by the GO treatment. GO-based treatment of cancerous cells demonstrates the potential of using nanomaterials as an effective carbon-based anti-cancer agent in the treatment of cancer.

Declarations

Acknowledgements: Authors would like to extend their sincere thanks to Natural and Medical Sciences Research Center, University of Nizwa, Oman. Authors would also like to extend their sincere appreciation to the Deanship of Scientific Research at King Saud University for funding this research group NO (RGP-271).

Author's contributions: Y.K.M. and P.R.R. were involved in the synthesis of GO nanosheets, antioxidant & MTT assays, and the preparation of the manuscript. K.B., D.D. helped in the characterization of GO and drafting the manuscript. A.H. AAA, and E.F. revised the manuscript, T.K.M.: drafted and revised the manuscript, AAH: analyzed the data and revised the manuscript. All the authors read and approved the final manuscript.

Conflicts of Interest: Authors declare that there is no conflict of interest among the co-authors.

References

1. F. Tonelli, V. Goulart, K. Gomes, M. Ladeira, A. Santos, E. Lorençon et al., Graphene-based nanomaterials : biological and medical applications and toxicity. Nanomedicine **10**(15), 2423–2450 (2015)
2. O. Akhavan, E. Ghaderi, Toxicity of Graphene and Graphene Oxide Nanowalls Against Bacteria. ACS Nano **4**(10), 5731–5736 (2010)
3. L. Feng, L. Wu, X. Qu, New Horizons for Diagnostics and Therapeutic Applications of Graphene and Graphene Oxide. 2013;168–86
4. D. Plach, J. Jampilek, Graphenic Materials for Biomedical Applications. Nanomaterials **9**, 1758 (2019)
5. G. Lalwani, A.M. Khan, B. Sitharaman, S. Brook, S. Brook, Toxicology of Graphene-Based Nanomaterials. Adv Drug Deliv Rev **105**(pt B), 109–144 (2016)
6. C. Liu, J. Zhao, R. Zhang, H. Li, B. Chen, L. Zhang et al., Multifunctionalization of graphene and graphene oxide for controlled release and targeted delivery of anticancer drugs. Am J Transl Res **9**(12), 5197–5219 (2017)
7. A.D. Garg, D.V. Krysko, P. Vandenabeele, P. Agostinis, Hypericin-based photodynamic therapy induces surface exposure of damage-associated molecular patterns like HSP70 and calreticulin. Cancer Immunol. Immunother. **61**, 215–221 (2012)
8. M. Grodzik, A. Winnicka, In vitro and in vivo effects of graphene oxide and reduced graphene oxide on glioblastoma. Int J Nanomedicine **10**, 1585–1596 (2015)
9. Y. Chang, S. Yang, J. Liu, E. Dong, Y. Wang, A. Cao et al. In vitro toxicity evaluation of graphene oxide on A549 cells. Toxicol Lett [Internet]. 2011;200(3):201–10. Available from: http://dx.doi.org/10.1016/j.toxlet.2010.11.016
10. M. Georgieva, B. Vasileva, G. Speranza, D. Wang, K. Stoyanov, M. Draganova-filipova et al., Amination of Graphene Oxide Leads to Increased Cytotoxicity in Hepatocellular Carcinoma Cells. Int J mol **21**, 2427 (2020)
11. M. Kutwin, E. Sawosz, S. Jaworski, M. Wierzbicki, B. Strojny, M. Grodzik et al., Nanocomplexes of Graphene Oxide and Platinum Nanoparticles against Colorectal Cancer Colo205, HT-29, HTC-116, SW480, Liver Cancer HepG2, Human Breast Cancer MCF-7, and Adenocarcinoma LNCaP and Human Cervical Hela B Cell Lines. Materials (Basel) **12**, 909 (2019)

12. K. Chen, Y. Huang, J. Chen. Understanding and targeting cancer stem cells : therapeutic implications and challenges. Nat Publ Gr [Internet]. 2013;34(6):732–40. Available from: http://dx.doi.org/10.1038/aps.2013.27
13. D. Bitounis, H. Ali-boucetta, B.H. Hong, D. Min, Prospects and Challenges of Graphene in Biomedical Applications. Adv Mater **26**(16), 2258–2268 (2013)
14. S.M. Mousavi, S.A. Hashemi, Y. Ghasemi, M. Amani, A. Babapoor, O. Arjmand. Applications of graphene oxide in case of nanomedicines and nanocarriers for biomolecules : review study. Drug Metab Rev [Internet]. 2019;0(0):1–30. Available from: https://doi.org/10.1080/03602532.2018.1522328
15. J. Shen, M. Shi, N. Li, B. Yan, H. Ma, Y. Hu et al., Facile Synthesis and Application of Ag-Chemically Converted Graphene Nanocomposite. Nano Res. **3**, 339–349 (2010)
16. H. Liu, S. Hu, Y. Chen, S. Chen, Characterization and drug release behavior of highly responsive chip-like electrically modulated reduced graphene oxide – poly (vinyl alcohol) membranes. J. Mater. Chem. **22**, 17311–17320 (2012)
17. L. Zhang, J. Xia, Q. Zhao, L. Liu, Z. Zhang, Functional Graphene Oxide as a Nanocarrier for Controlled Loading and Targeted Delivery of Mixed Anticancer Drugs. Small **6**(4), 537–544 (2010)
18. J. Liu, L. Cui, D. Losic. Graphene and graphene oxide as new nanocarriers for drug delivery applications. Acta Biomater [Internet]. 2013;9(12):9243–57. Available from: http://dx.doi.org/10.1016/j.actbio.2013.08.016
19. P. Huang, C. Xu, J. Lin, C. Wang, X. Wang, C. Zhang et al., Folic Acid-conjugated Graphene Oxide loaded with Photosensitizers for Targeting Photodynamic Therapy. Theranostics **1**, 240–250 (2011)
20. N.I. Zaaba, K.L. Foo, U. Hashim, S.J. Tan, W. Liu, C.H. Voon. Synthesis of Graphene Oxide using Modified Hummers Method : Solvent Influence. Procedia Eng [Internet]. 2017;184:469–77. Available from: http://dx.doi.org/10.1016/j.proeng.2017.04.118
21. A. Bellova, E. Bystrenova, M. Koneracka, P. Kopcansky, F. Valle, N. Tomasovicova et al., Effect of Fe(3)O(4) magnetic nanoparticles on lysozyme amyloid aggregation. Nanotechnology **21**(6), 65103 (2010 Feb)
22. Q. Yuan, G. Zhou, L. Liao, Y. Liu, L. Luo, Interfacial structure in AZ91 alloy composites reinforced by graphene nanosheets. Carbon N Y **127**, 177–186 (2017)
23. L. Bokobza, Some Applications of Vibrational Spectroscopy for the Analysis of Polymers and Polymer Composites. 2019
24. B. Ossonon, D. Bélanger, Synthesis and characterization of sulfophenyl-functionalized reduced graphene oxide sheets. RSC Adv **7**(44), 27224–27234 (2017)
25. S.M. Bhagyaraj, O.S. Oluwafemi. Nanotechnology : The Science of the Invisible. In: Synthesis of Inorganic Nanomaterials [Internet]. Elsevier Ltd.; 2018. p. 1–18. Available from: http://dx.doi.org/10.1016/B978-0-08-101975-7.00001-4
26. D. Titus, E.J.J. Samuel, S.M. Roopan. Nanoparticle characterization techniques [Internet]. Green Synthesis, Characterization and Applications of Nanoparticles. Elsevier Inc.; 2019. 303–319 p.

Available from: https://doi.org/10.1016/B978-0-08-102579-6.00012-5

27. S. Zhang, J. Li, G. Lykotrafitis, G. Bao, S. Suresh, Size-Dependent Endocytosis of Nanoparticles. Adv Mater **21**, 419–424 (2009)
28. J. Linares, M. Concepcio, P.A.A.P. Marques, M.T. Portole, Endocytic Mechanisms of Graphene Oxide Nanosheets in Osteoblasts, Hepatocytes and Macrophages. ACS Appl Mater Interfaces **6**, 13697–13706 (2014)
29. E. Fröhlich, The role of surface charge in cellular uptake and cytotoxicity of medical nanoparticles. Int J Nanomedicine. 2012;5577–91
30. Q. Yang, W. Zhongying, A.C.E. Owensa, I. Kulaotsa, Y. Chen, A.B. Kane et al., Antioxidant Chemistry of Graphene-Based Materials and its Role in Oxidation Protection Technology. Nanoscale **6**(20), 11744–11755 (2015)
31. Y. Lee, Y. Yoon, H. Yoon, S. Song, H. Park, Y.Y. Lee et al., Enhanced Antioxidant Activity of Bioactives in Colored Grains by Nano-Carriers in Human Lens Epithelial Cells. Molecules **23**, 1327 (2018)
32. M.S. Blois, Antioxidant determinations by the use of a stable free radical. Nature **181**, 1199–1200 (1958)
33. D. Suresh, M.A.P. Kumar, H. Nagabhushana, S.C. Sharma. Cinnamon supported facile green reduction of graphene oxide, its dye elimination and antioxidant activities. Mater Lett [Internet]. 2015;151:93–5. Available from: http://dx.doi.org/10.1016/j.matlet.2015.03.035
34. R. Rajeswari, H.G. Prabu. Synthesis Characterization, Antimicrobial, A., and Cytotoxic Activities of ZnO Nanorods on Reduced Graphene Oxide. J Inorg Organomet Polym Mater [Internet]. 2017;0(0):0. Available from: http://dx.doi.org/10.1007/s10904-017-0711-9
35. L. Elias, R. Taengua, B. Frígols, B. Salesa, Á Serrano-Aroca, Carbon Nanomaterials and LED Irradiation as Antibacterial Strategies against Gram-Positive Multidrug-Resistant Pathogens. Int J Mol Sci. 2019 Jul;20(14)
36. S. Gurunathan, J. Han, J. Park, J. Kim, An in vitro evaluation of graphene oxide reduced by Ganoderma spp. in human breast cancer cells (MDA-MB-231). Int J Nanomedicine **9**(1), 1783–1797 (2014)
37. J. Wu, R. Yang, L. Zhang, Z. Fan, S. Liu, Cytotoxicity effect of graphene oxide on human MDA-MB-231 cells. Toxicol Mech Methods **25**(4), 312–319 (2015)
38. H. Cheng, Y. Bo, W. Shen, X. Ren, J. Tan, Z. Jia et al., Longikaurin E induces apoptosis of pancreatic cancer cells via modulation of the p38 and PI3K/AKT pathways by ROS. Naunyn Schmiedebergs Arch Pharmacol **388**(6), 623–634 (2015 Jun)

Figures

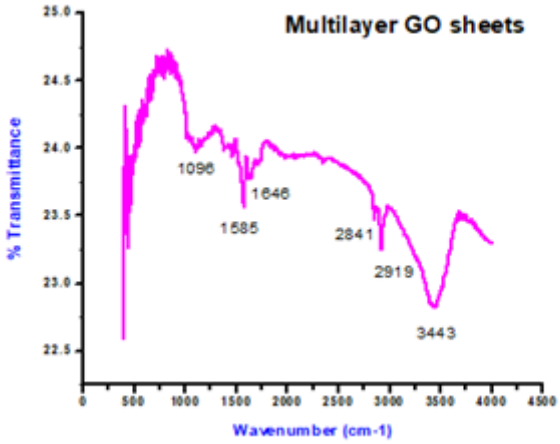

Figure 1

FT-IR of graphene oxide nanosheet.

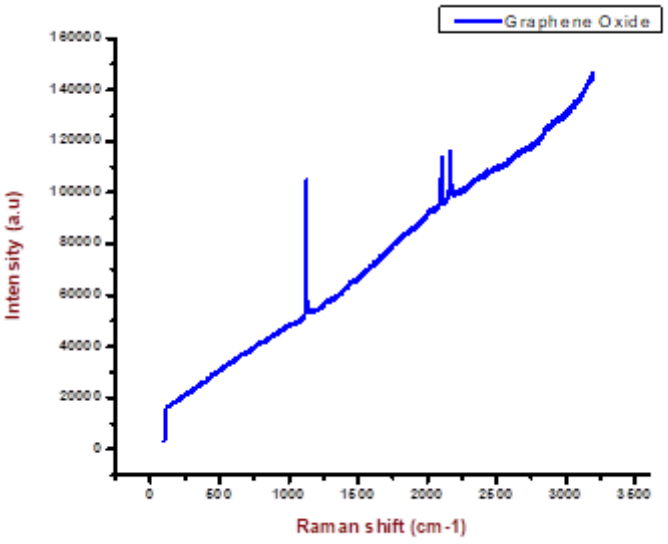

Figure 2

Raman spectroscopy plot of graphene oxide nanosheet.

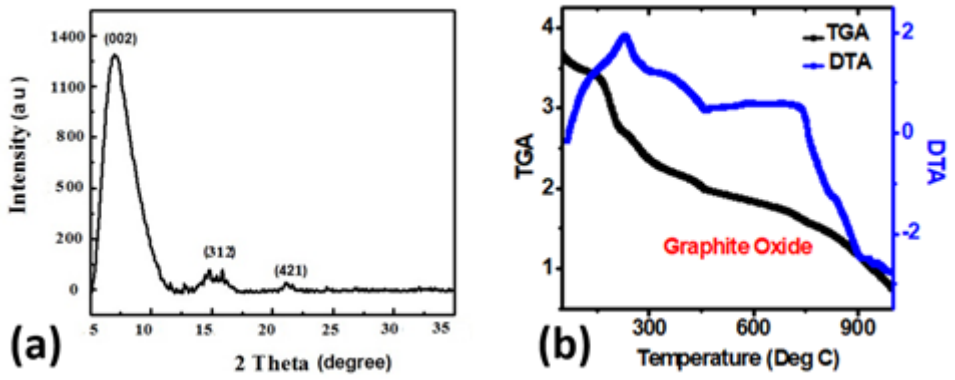

Figure 3

a). XRD spectroscopy plot of graphene oxide nanosheet; b) TGA of GO sheets.

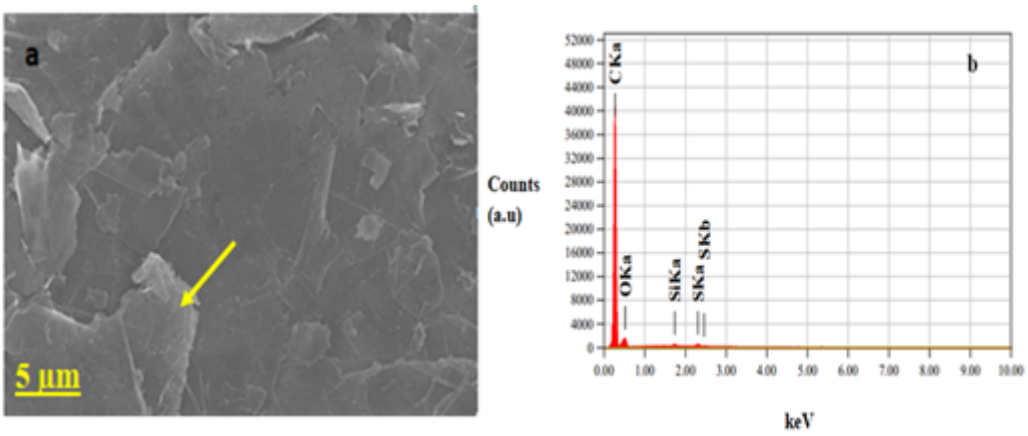

Figure 4

(a) FESEM and (b) EDAX of graphene oxide nanosheet.

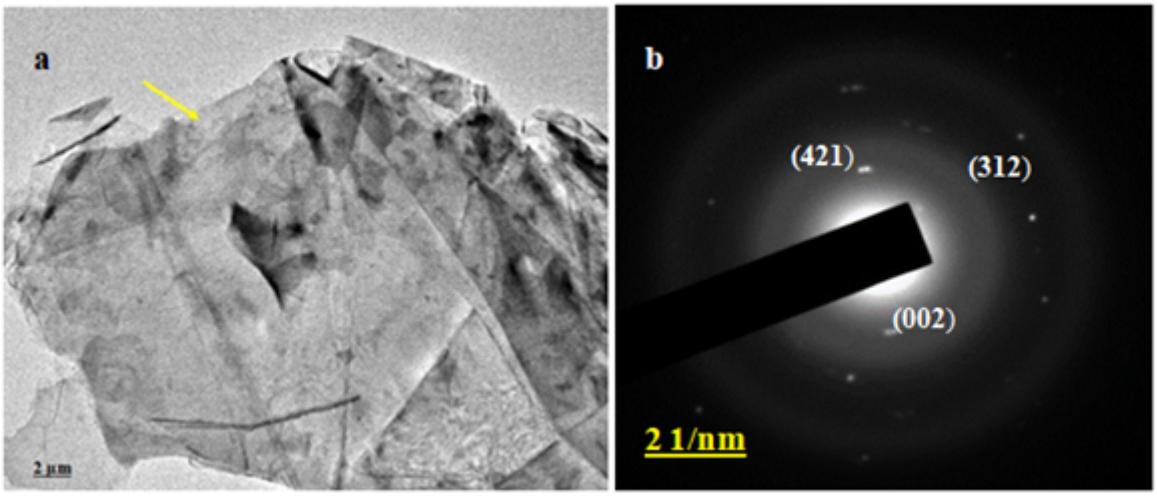

Figure 5

HR-TEM of graphene oxide nanosheets; b) SAED of GO sheets indicating crystalline lattices.

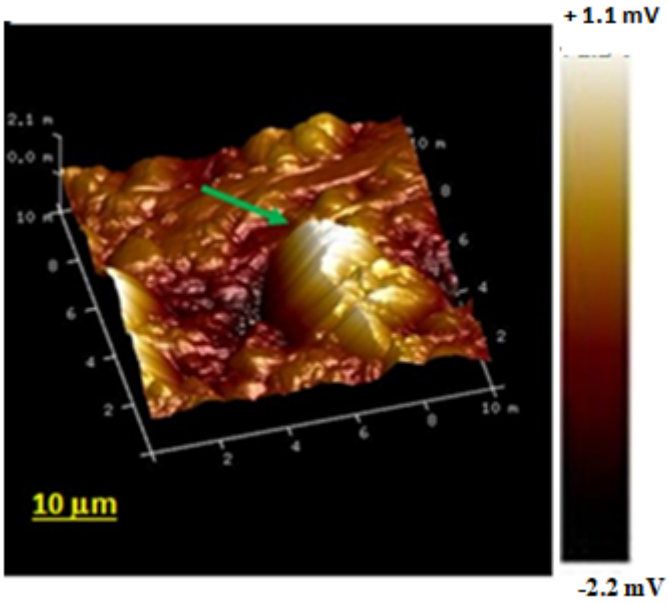

Figure 6

AFM of graphene oxide nanosheets.

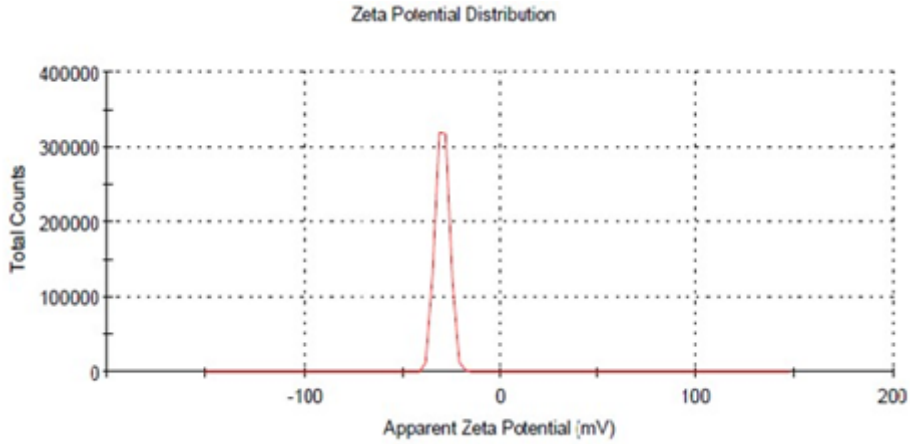

Figure 7

DLS of graphene oxide nanosheets.

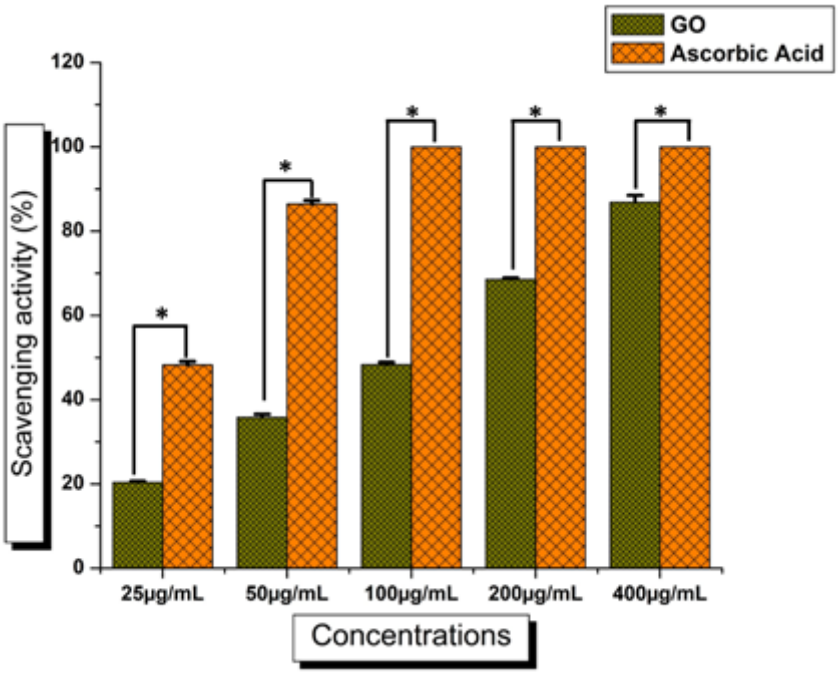

Figure 8

DPPH radical scavenging assay of graphene oxide nanosheet. Error bar represents standard deviation of mean. *$p \leq 0.05$. Significant difference ($p \leq 0.05$) within a parameter between two lines is denoted by asterisk.

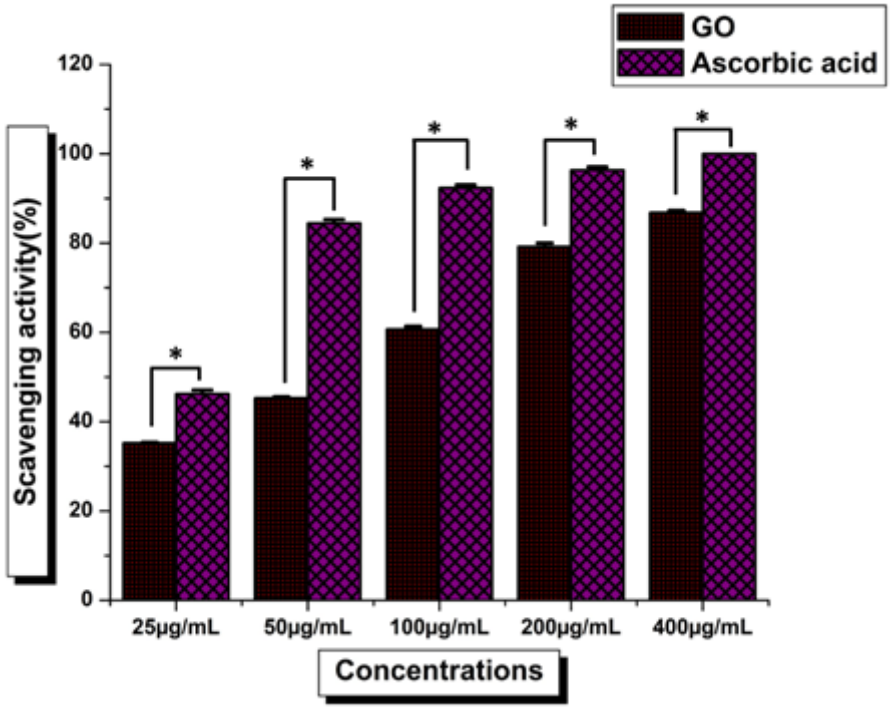

Figure 9

H2O2 radical scavenging assay of graphene oxide nanosheet. Error bar represents standard deviation of mean. *p ≤ 0.05. Significant difference (p ≤ 0.05) within a parameter between two lines is denoted by asterisk.

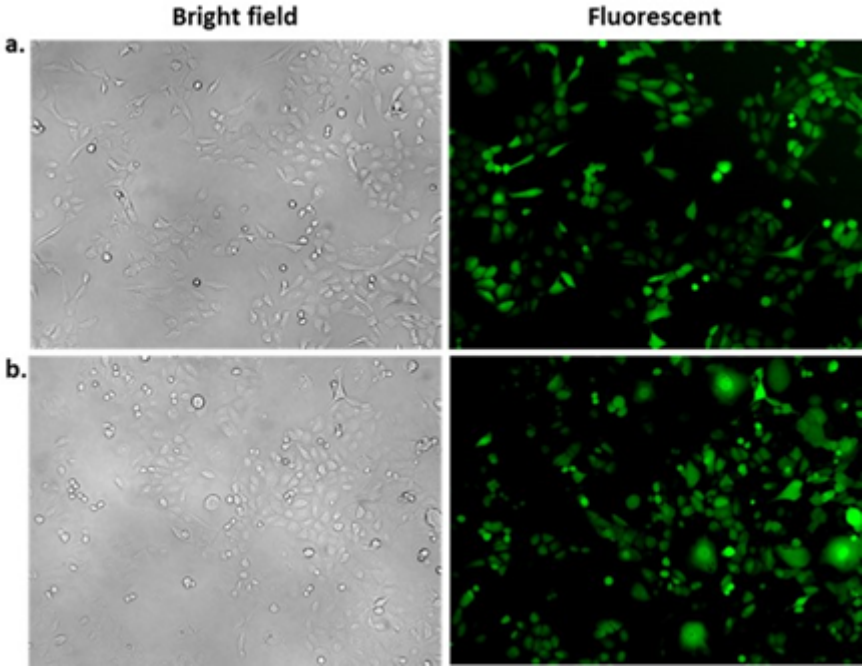

Figure 10

Fluorescence and bright field images of GFP-tagged MDA-MB-231 cells showed internalization of GOs at different time intervals; (a) Control MDA-MB-231 [10X], (b) GO treated MDA-MB-231after 48 hrs [10X].

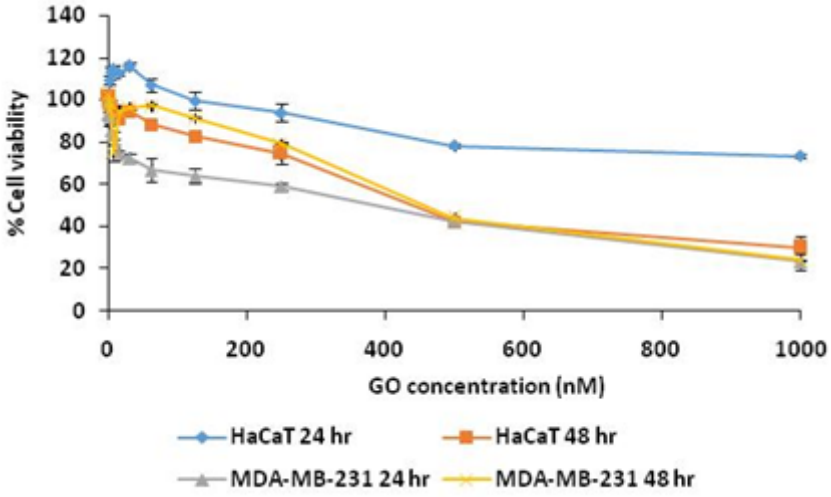

Figure 11

Cell viability of MDA-MB-231 and HaCaT after treatment with different concentrations of GO nano formulations after 24 hr and 48 hr.

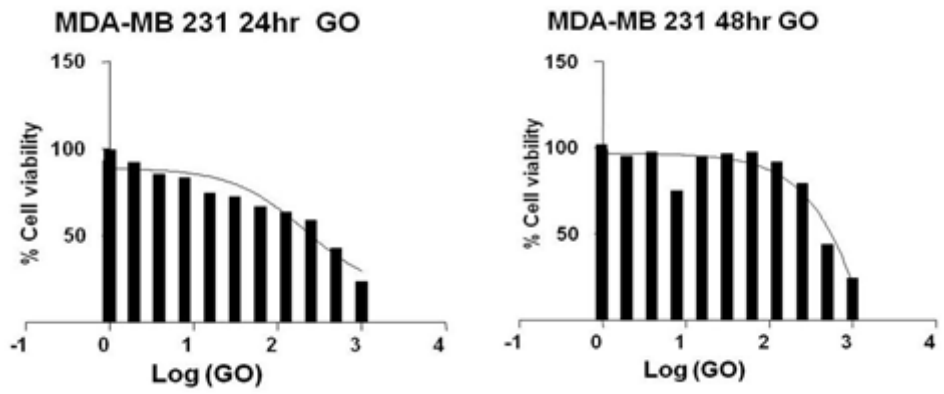

Figure 12

Cell viability assay of (a) GO treated MDA-MB-231 cell lines [24 hr post incubation] and (b) GO treated MDB-MB-231 [48 hr post incubation].

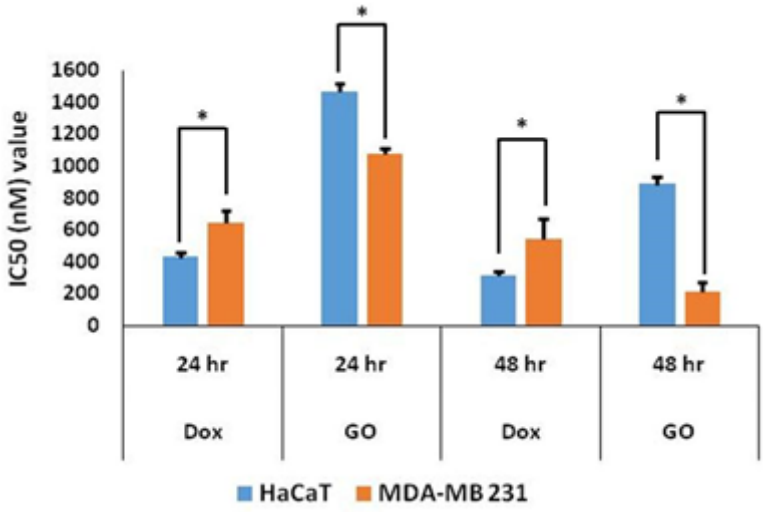

Figure 13

Cell viability [IC 50 value] of MDA-MB-231, HaCaT, after treatment with different nano formulations [Dox: Doxorubicin [control], GO nanosheets] after 24 hr and 48 hr. Error bar represents standard deviation of mean. *$p \leq 0.05$. Significant difference ($p \leq 0.05$) within a parameter between two lines is denoted by asterisk.